Canadian Mineralogist
Vol. 22, pp. 565-575 (1984)

OURAYITE FROM IVIGTUT, GREENLAND

EMIL MAKOVICKY
Institute of Mineralogy, University of Copenhagen, Østervoldgade 10, 1350 Copenhagen K, Denmark

SVEN KARUP-MØLLER
Institute of Mineral Industry, Technical University of Denmark, 2800 Lyngby, Denmark

ABSTRACT

In fine-grained ore fragments from the Ivigtut cryolite deposit (Greenland), ourayite is associated with berryite, aikinite, galena, matildite, chalcopyrite, pyrite, native Bi and Au. Originally, ourayite crystallized as $Our_{71.6}$, but it later exsolved into lamellae of $Our_{\sim 80}$ in a matrix of $Our_{68.5}$. Ourayite$_0$ is defined as $Pb_{10}Bi_2S_{13}$, ourayite$_{100}$ as $PbBi_{6.5}Ag_{4.5}S_{13}$. The matrix *ourayite* is *B*-centred orthorhombic, with *a* 13.49(2), *b* 44.17(4), *c* 4.05(2) Å, space group *Bbmm* or *Bb*2_1*m*. It is close to the ideal composition $Pb_4Ag_3Bi_5S_{13}$ ($Our_{66.67}$). The exsolved phase is present as coherent (100) lamellae. It is *P-ourayite,* also orthorhombic but primitive, *a* 13.15(2), *b* 44.17(4), *c* 4.05(2) Å; the probable space-group is *Pbnm* (D_{2h}^{16}) or *Pbn*2_1 (C_{2v}^9). Its empirical formula, $Pb_{2.8}Ag_{3.6}Bi_{5.6}S_{13}$ (Our_{80}), represents a compromise, based on microprobe data, its modal proportion and crystal-chemistry considerations. The Ag–Pb–Bi sulfosalts of the lillianite homologous series from Ivigtut all preserve nearly the same molar (Ag + Bi)/Pb ratio.

Keywords: ourayite, sulfosalt, exsolution, Ivigtut, Greenland, lillianite, cryolite.

SOMMAIRE

On trouve l'ourayite dans des fragments de minerai de cryolite à granulométrie fine du gîte d'Ivigtut (Groënland); lui sont associées: berryite, aikinite, galène, matildite, chalcopyrite, pyrite, bismuth et or natifs. De composition $Our_{71.6}$ à l'origine, elle s'est transformée par exsolution en une matrice de $Our_{68.5}$ avec des lamelles de $Our_{\sim 80}$. Les pôles de la solution solide sont: $Our_0 = Pb_{10}Bi_2S_{13}$ et $Our_{100} = PbBi_{6.5}Ag_{4.5}S_{13}$. L'ourayite de la matrice est orthombique à face *B*-centrée, avec *a* 13.49(2), *b* 44.17(4), *c* 4.05(2) Å, groupe spatial *Bbmm* ou *Bb*2_1*m*, et se rapproche de la composition idéale $Pb_4Ag_3Bi_5S_{13}$ ($Our_{66.67}$). La phase exsolvée forme des lamelles cohérentes (100). C'est l'ourayite-*P,* orthorhombique elle aussi, mais primitive, *a* 13.15(2), *b* 44.17(4), *c* 4.05(2) Å, groupe spatial probable *Pbnm* (D_{2h}^{16}) ou *Pbn*2_1 (C_{2v}^9). Sa formule empirique, $Pb_{2.8}Ag_{3.6}Bi_{5.6}S_{13}$ (Our_{80}), est idéalisée d'après les données à la microsonde, sa proportion modale et des considérations cristallochimiques. Les sulfosels à Ag, Pb et Bi de la série des homologues de la lillianite d'Ivigtut possèdent à peu près le même rapport molaire (Ag + Bi)/Pb.

(Traduit par la Rédaction)

Mots-clés: ourayite, sulfosel, exsolution, Ivigtut (Groënland), lillianite, cryolite.

INTRODUCTION

The cryolite deposit at Ivigtut, south Greenland is the type locality for a number of lillianite homologues (Karup-Møller 1970, 1973, Makovicky & Karup-Møller 1977a, b). These minerals occur in late, fine-grained sulfosalt – galena associations (Karup-Møller 1973, Karup-Møller & Pauly 1979). This paper describes the occurrence of *ourayite,* an additional homologue of lillianite from Ivigtut that we described from Old Laut's mine, Colorado in 1977 (specimen ROM 4100).

The *lillianite homologous series* comprises Pb–Bi–Ag sulfosalts with crystal structures composed of layers of a galena-like structure that is regularly twinned by a reflection operation on $(311)_{PbS}$. On the twin and composition planes, the co-ordination octahedra of metals coalesce and are replaced by bicapped trigonal co-ordination prisms occupied by Pb. Therefore, the composition of phases in this homologous series depends on the spacing of the twin planes. Makovicky & Karup-Møller (1977a) proposed a designation of homologues of lillianite according to the number N_1 and N_2 of octahedra strung diagonally across two adjacent slabs of galena-like structure around a twin plane. The general chemical formula of a lillianite homologue depends on the average thickness of the slab, expressed by the value of $N = (N_1 + N_2)/2$, and reads $M_{N+1}S_{N+2}$. If the substitution Ag + Bi $\rightleftarrows$ 2 Pb that is typical for the octahedral positions in the homologues of lillianite is incorporated, the general formula becomes $Pb_{N-1-2x}Bi_{2+x}Ag_xS_{N+2}$. The composition of the lillianite homologue can also be expressed as the percentage of the "fully substituted" end-member in which all octahedral positions are occupied by Ag and Bi so that $x = (N-2)/2$. The difference from 100% will represent the percentage of the Ag-free end member $Pb_{N-1}Bi_2S_{N+2}$. Details of the calculation procedures for N, x and the percentage of substitution, based on the proportion of Pb, Bi and Ag, are given in Makovicky & Karup-Møller (1977a).

In 1976 and 1978, Mr. L. Andersen, a mineral collector from Copenhagen, found three fragments of ore measuring less than 2 × 4 × 8 cm at the former stockpile of the cryolite refinery in Copenhagen.

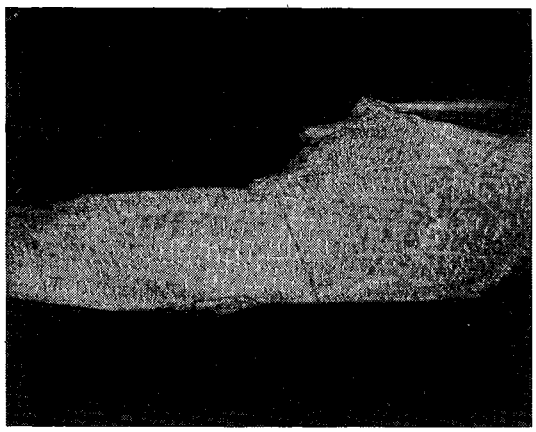

FIG. 1. Ourayite lath in fluorite with exsolved lenticular bodies of Ag–Bi-enriched ourayite. Etched with concentrated HNO_3; plane-polarized light, 195×.

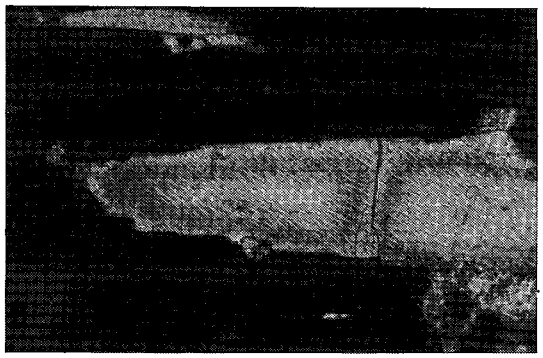

FIG. 2. Ourayite lath with exsolved Ag–Bi-enriched ourayite. Same conditions as in Figure 1; different crystallographic orientation of the section through the host crystal.

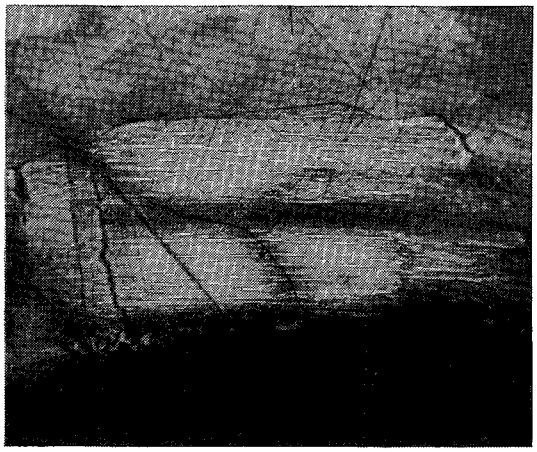

FIG. 3. Ourayite crystal with exsolved Ag–Bi-enriched phase. Lamellae are parallel to the elongation of the host; conditions as in Figure 1, 215×.

These specimens, denoted as 191/1976, 29/1978 and 30/1978, are deposited in the collections of the Geological Museum, Copenhagen. The specimens are characterized by black, coarse-grained cryolite crosscut and partly replaced by fine-grained fluorite and topaz, with about 20% of disseminated sulfosalts. The origin of the ore specimens remains unknown, but they most likely come from breccia zones associated with greisen in the southern border-zone of the deposit (H. Pauly, per. comm.).

The ore specimens differ from those of the gustavite – cosalite – galena (Karup-Møller 1973) and the galena – matildite – aikinite associations (Karup-Møller & Pauly 1979) by the presence of black cryolite. Those two associations were found in, or close to, the fluorite zone of the deposit. All three associations contain fluorite – topaz aggregates with disseminated sulfosalts.

Optical Properties

Ourayite has optical properties that are practically indistinguishable from those of other Ag–Bi–Pb homologues of lillianite (Vendrell-Saz *et al.* 1978, Karup-Møller 1977). Extinction is found to be parallel to elongation, although the broad maximum in extinction angle makes observations difficult. Ourayite forms platy acicular crystals up to one millimetre across (Fig. 1). Their internal structure is complex owing to (multiple) exsolution, best revealed by etching with concentrated HNO_3 for about 10 seconds.

A fine-grained exsolved phase is evenly distributed in the matrix of ourayite crystals. Individual grains are aligned parallel. According to the orientation of the section through the host crystal, the grains may appear as lamellae (in cases branched) parallel to elongation of the host crystal, as obliquely arranged lenticular bodies, or as short wavy lenses that are perpendicular to the elongation of the section through the host crystal (Figs. 1–3). Furthermore, in the sections in which the exsolved phase has a lenticular character, alternating lamellae parallel to the elongation of the host crystal are, respectively, more and less intensely etched. They resemble polysynthetic twinning, but on close examination they represent areas with lower and higher content, respectively, of lenticular exsolution-lamellae. Wherever distinguishable, the exsolved phase exhibits extinction parallel to that of the matrix, but the hue of the blue and brown anisotropy differs.

Chemical Data

The chemical composition of the complex aggregates of ourayite was determined by means of an electron microprobe using the following analytical wavelengths and standards: Ag$L\alpha$ (pure Ag),

Cu$K\alpha$ (pure Cu), Bi$K\alpha$ (pure Bi), Pb$L\alpha$ and S$K\alpha$ (natural galena). No Sb was detected. The first round of analyses, comprising ourayite, berryite, aikinite and associated galena in the polished sections 29/1978, 30/1978 and 191/1976, was performed on a Hitachi XMA – 5B microprobe at the Institute of Mineralogy, University of Copenhagen. Springer's (1967) correction program was used, modified after Sweatman & Long (1969) by J. Rønsbo. Detailed chemical variations in ourayite were studied using a JEOL Superprobe 733 apparatus at the same institute. In this case, corrections were performed using the JEOL PACM program set.

Because of indistinct optical properties and the fine-grained character of exsolution products, it was not possible to clearly discern them from the ourayite matrix in the microscope of the microprobe apparatus. Therefore, the sets of point analyses that are considered here were obtained at random. The overall means represent the composition estimates for the entire crystals before exsolution, whereas the Pb-rich and (Ag + Bi)-rich extremes, respectively, approach the compositions of the matrix and the exsolved phase (Table 1; Figs. 4, 5).

The average composition of ourayite before exsolution (Table 1) ranges from 70.7 to 72.2% of the Ag–Bi end member and centres about the value 71.6% obtained for 65 measurements on the sample 29/78 using the JEOL Superprobe. This value is somewhat higher than that found in the original ourayite by Makovicky & Karup-Møller (1977b), 69.7%. Although the calculated values of N range from 9.7 to 10.4, we shall here use the only crystallographically acceptable value of N, which is equal to 11. Lower values of N lead to unacceptable dimensions of the metal co-ordination octahedra in the structure with the present cell-parameters (Makovicky 1977). The systematic error in the microprobe analyses that causes the above difference of chemically and crystallographically determined values of N is commensurate in the compositional triangle Pb–Ag–Bi with that observed on gustavite and related phases (Karup-Møller 1977, Makovicky & Karup-Møller 1977b). Presumably, it represents an artefact of the procedures used in correcting microprobe data. For the average extent of substitution quoted above, the ideal composition of ourayite before exsolution was $Pb_{3.56}Ag_{3.22}Bi_{5.22}S_{13}$, as compared with $Pb_{3.72}Ag_{3.14}Bi_{5.14}S_{13}$ for the type material from Ouray, Colorado.

The more-or-less compact groups of analytical data-points on the Pb-rich side of data-point clusters indicate that the extent of substitution is in the range 68.5–70.3. For the lowest value, the ideal formula is $Pb_{3.84}Ag_{3.08}Bi_{5.08}S_{13}$, close to $Pb_4Ag_3Bi_5S_{13}$ ($Pb_{16}Ag_{12}Bi_{20}S_{52}$), which itself represents a simpler ideal formula for ourayite than given by Makovicky & Karup-Møller (1977b); it corresponds to a degree of substitution of 66.67%.

The compositions with the highest extent of (Ag + Bi) substitution are much more scattered along the line with N constant. The highest (Ag + Bi)-substituted average composition corresponds to 75.1% substitution (Table 1); the highest individual point-analysis represents $^{9.8}L_{77.8}$. The total difference in the extent of substitution between the matrix and the lamellae appears to be rather small when the large difference in the a parameter between the two exsolved phases is considered. Therefore, alternative ways were sought that would furnish additional data

TABLE 1. AVERAGED MICROPROBE DATA FOR OURAYITE FROM IVIGTUT

Sample	Meas. points	Ag*	Cu*	Pb*	Bi*	S*	Total	Ag+	Cu+	Pb+	Bi+	S+	N	%
191/76T	18	12.3(4)	0.4(2)	28.7(13)	42.9(10)	16.6(3)	100.9(8)	24.5	1.4	29.9	44.2	111.2	9.9	71.5
191/76P	5	12.1(4)	0.3(2)	29.3(4)	42.3(9)	16.5(2)	100.6(7)	24.4	0.9	30.7	44.0	111.9	9.7	70.3
191/76A	4	12.6(4)	0.5(2)	26.3(5)	44.1(3)	16.4(2)	100.0(30)	25.3	1.7	27.4	45.6	110.2	9.8	74.8
29/78T	25	11.9(6)	0.9(3)	28.4(13)	43.2(11)	16.9(2)	101.3(14)	23.5	3.2	29.2	44.1	112.8	10.4	72.2
29/78P	5	11.6(4)	1.0(1)	30.0(3)	42.4(10)	16.9(3)	101.9(8)	23.0	3.2	30.8	43.1	112.1	10.7	70.1
29/78A	6	12.4(6)	0.7(4)	26.2(10)	44.2(6)	16.9(1)	100.5(22)	24.7	2.5	27.3	45.5	113.6	10.0	75.0
30/78T	7	11.6(3)	0.6(2)	28.6(8)	41.7(8)	16.6(1)	99.1(10)	23.6	2.1	30.4	43.9	113.6	10.0	70.7
30/78P	4	11.5(3)	0.5(2)	29.0(4)	41.4(3)	16.5(2)	98.9(13)	23.5	1.7	31.0	43.8	114.0	9.8	69.9
29/78mT	65	11.2(4)	1.0(2)	28.7(12)	43.2(9)	17.6(2)		22.2	3.5	29.8	44.5	117.8	9.7	71.6
29/78mP	7	10.7(3)	0.8(1)	30.5(3)	41.8(5)	17.4(2)		21.6	2.8	32.0	43.5	118.3	9.5	68.5
29/78mA	7	11.5(5)	1.3(2)	26.5(9)	44.6(6)	17.6(1)		22.8	4.4	27.3	45.6	117.3	9.9	75.1

Standard deviations are indicated in parentheses in terms of the last digit. Sb not detected. * Data expressed in weight %. + Data expressed in atomic proportions, $\Sigma Me = 100$. N is the average order number of the lillianite homologue, based on the chemical composition; % is the percentage of Ag-Bi substitution. m indicates the detailed measurements made on the JEOL Superprobe 733. T, P and A, respectively, indicate the overall average and the partial average of the most Pb-rich and most (Ag+Bi)-rich compositions.

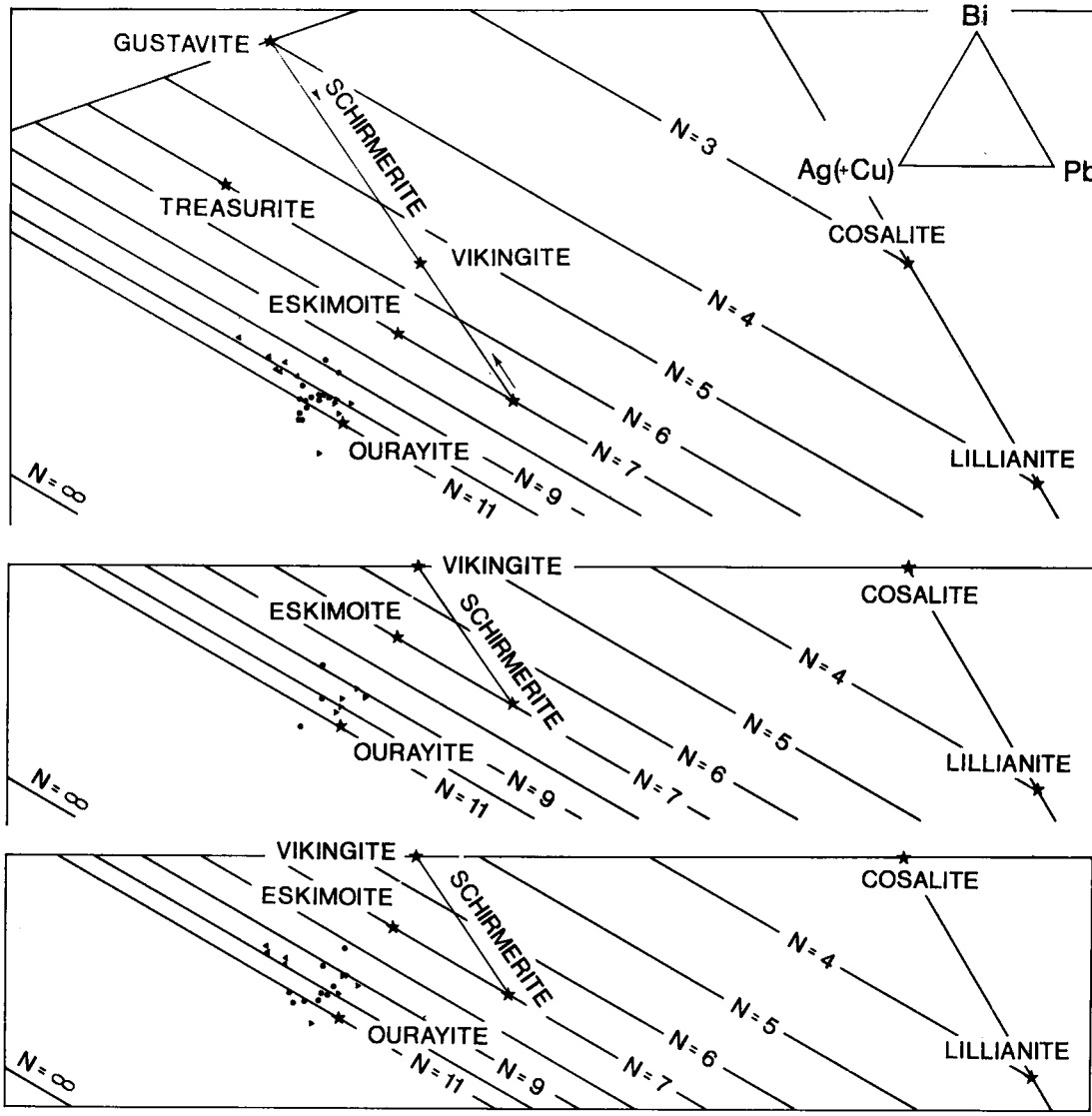

FIG. 4. Portion of the compositional triangle Ag–Pb–Bi (*i.e.*, Ag_2S–Bi_2S_3–Pb_2S_2) with the point compositions of the ourayite exsolution-intergrowths plotted relative to the isopleths of the *N* values of the lillianite homologous series. The upward-pointing triangles denote the data approximating the composition of the Ag–Bi-rich exsolved phase; the downward-pointing triangles, that of the Pb-rich matrix; circles represent the remaining data (at.%). Hitachi X7A–5B microprobe. Ideal compositions of lillianite homologues, denoted by stars, are taken from Makovicky & Karup-Møller (1977b).

and allow further constraints to be placed on the composition of the minor exsolved phase. They will be described and results evaluated after presentation of the X-ray data on ourayite.

X-RAY CRYSTALLOGRAPHY

Five crystals were extracted from the polished sections and studied on a Weissenberg apparatus. All of them display the same characteristics, indicating homogeneity of the sulfosalt studied. The quality of single-crystal X-ray photographs is invariably rather poor (smear of reflections, several subparallel domains, intergrowth with additional, unidentified phases), similar to the situation encountered with the original material from Old Laut's mine, Colorado (Makovicky & Karup-Møller 1977b).

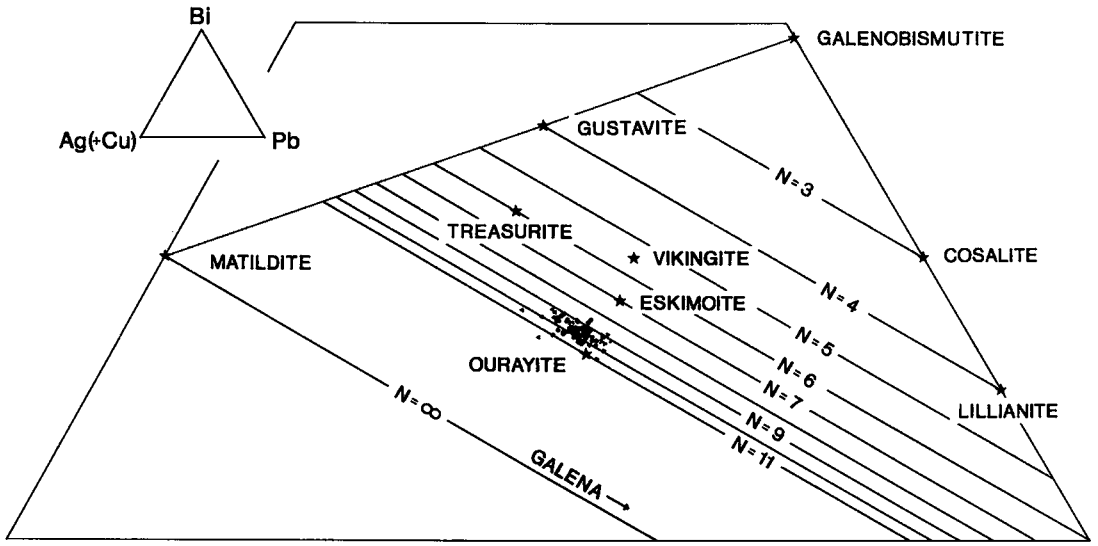

FIG. 5. Analytical data for the sample 191/76 obtained using JEOL Superprobe 733. For details, see Figure 7 (at. %).

Two orthorhombic ourayite phases are present in all the cases studied, in perfectly parallel exsolution with common $\vec{a}$, $\vec{b}$ and $\vec{c}$ vectors. Within the accuracy of Weissenberg and rotation photographs, the *b* and *c* parameters of both phases are identical, whereas there is an appreciable difference in the respective *a* parameters. From the quartz-calibrated zero-level Weissenberg photographs and rotation photographs prepared using Cu$K\alpha$ radiation, the following cell-parameters were obtained. The principal, *B-centred* phase has *a* 13.49(2), *b* 44.17(4) and *c* 4.05(2) Å. The minor phase, with a *primitive* unit-cell, has *a* 13.15(2), *b* 44.17(4) and *c* 4.05(2) Å.

Whereas the *b* parameter does not display visible variation, the *a* parameter of both the major and the minor phases shows a certain amount of variation, indicating a (partly) incomplete exsolution. The high-2θ *hkl* reflections with $|k|$ equal to or close to zero are smeared out along the $\Delta 2\theta$ direction to such an extent that a single elongate spot is formed from α_1 and α_2 reflections. In two less perfectly exsolved crystals of ourayite with less distinct reflections of the minor phase, the Δa difference is less than the value of 0.34 Å displayed by the well-exsolved crystals, the *a* parameter of the minor phase being slightly closer to that of the main component.

No multiplicity of the 4 Å parameter is observable on well-exposed rotation photographs. The diffraction symmetry of the principal component is *mmmBb*** which, together with the identity of relevant intensities on the *hk*0 and *hk*2 levels of the reciprocal lattice, limits the choice in space group to *Bbmm* and *Bb*2_1*m*. The results for the minor phase are not so unambiguous owing to the combination of the weakness of its reflections with the occurrence of the pronounced "lillianite-type" areas of low and high intensities in the reciprocal lattice of ourayite (*cf.* Makovicky & Karup-Møller 1977a). The lillianite-type pattern of intensities implies an $h + l = 2n$ pattern of strong intensity values (rows) in the slice of the reciprocal lattice along (010)* plane so that in the $h + l = (2n + 1)$ rows, all reflections with low-to-zero $|k|$ values have intensities close or equal to zero. Thus, no violation of the $h + l = 2n$ could be observed for the *hk*0, *hk*1 or *hk*2 levels, but it cannot be confirmed that this is due to systematic glide-extinctions alone. Therefore, the preferred diffraction-symmetry is *mmmPbn*, which allows the space groups *Pbnm* or *Pbn*2_1 (the former supported by the probable equality of the relevant *hk*0 and *hk*2 reflections). The less likely alternative is *mmmPb***, which gives *Pbmm*, *Pbm*2 or *Pb*2_1*m* as the possible space-groups.

The powder pattern of the Ivigtut ourayite (Table 2) was prepared using a Gandolfi camera and one of the crystals examined. Although the character of the reciprocal lattice (the lillianite-type regions of tightly clustered strong reflections) precludes cell-parameter refinement based on normal-resolution powder photographs, the principal lines of the pattern were indexed using the calculated *d*-values of the strong reflections in the Weissenberg photographs.

The reciprocal lattice of the principal, *B*-centred ourayite component from Ivigtut is identical to that of the type ourayite from Old Laut's mine, Ouray, Colorado (Makovicky & Karup-Møller 1977b). The cell parameters of the type material, which does not

TABLE 2. X-RAY POWDER-DIFFRACTION DATA FOR OURAYITE FROM IVIGTUT

I est	d obs	d calc	hkl	I est	d obs	d calc	hkl
3	4.15	4.16	340	5	2.029	2.027	002
2	3.74	3.75	131			2.025	012
1	3.60	3.66	141, 370	2	1.996	1.996	122
		3.55	151, 061	1	1.838	1.840	0.24.0, 3.19.1
9	3.42	3.45	2.11.0			1.841	322
		3.43	161, 221	3	1.781		
9	3.31	3.31	171, 390, 241	4	1.732		
1	3.22	3.22	440	3	1.660		
2	3.04	3.04	271	1	1.436		
		3.03	2.13.0	1	1.359		
10	2.8678	2.877	1.15.0, 480	2	1.321		
		2.857	2.14.0	2	1.288		
1	2.149	2.150	660	1	1.194		
		2.148	561	1	1.173		
4	2.080	2.082	680	1	1.106		
		2.080	2.17.1, 581, 1.12.0				

Debye-Scherrer camera, circumference 180 mm, sample 30/78.

even exhibit traces of reflections of the exsolved phase, were determined from the single-crystal photographs of rather poor crystals as *a* 13.46, *b* 44.04, *c* 4.10 Å. They do not significantly differ from the present results. As was the case in the Ouray sample, the rows of the reciprocal lattice parallel to *b* are in the areas of strong or medium reflections underlain by weak continuous streaks, which indicate partial structural disorder (slab-thickness faults).

Alternative Estimates of Composition of Ourayite

The minuteness of the exsolved lenticular or lamellar bodies of the minor ourayite phase prevents its reliable microprobe analysis. Furthermore, these bodies may not be quite homogeneous, as was the case for the minor exsolved component in gustavite from Ivigtut (Karup-Møller 1970).

In the case of the gustavite – lillianite exsolution pair, Makovicky & Karup-Møller (1977b) used changes in cell parameters connected with the Ag + Bi $\rightleftarrows$ 2Pb substitution to estimate the composition of the exsolved phase. For ourayite, however, only one known composition with measured cell-parameters exists. Therefore, extrapolation of data from the gustavite – lillianite series (N = 4), heyrovskyite solid-solution series (N = 7) and the galena – matildite series ($N = \infty$) was attempted. The applicability of these data may be limited *a priori* because the volume change in the ourayite series proceeds differently than in all these series. Comparison with the andorite – fizelyite series, in which the volume change proceeds in the same way as in ourayite, *i.e.*, by means of Δa, is hampered by the difference between the dimensions of the Bi and Sb co-ordination polyhedra.

If possible problems in calibration and departures from linearity are ignored, the cell-parameter data for gustavite$_{100}$ (Harris & Chen 1975) and for lillianite Gu$_{12.5}$ from Uludag (Turkey) (Makovicky & Karup-Møller 1977b) yield an estimate of the cell-volume change for the entire substitution range ($Pb_3Bi_2S_6 \rightarrow PbAgBi_3S_6$, *i.e.*, Gu$_0$ → Gu$_{100}$) of -46.01 Å^3. From the data by Klomínský *et al.* (1971) on heyrovskyite Hey$_{8.4}$ and those by Karup-Møller & Makovicky (1981) on (Ag + Bi)-substituted heyrovskyite Hey$_{71.1}$, the same change (from $Pb_6Bi_2S_9$ to $PbAg_{3.5}Bi_{5.5}S_{11}$, *i.e.* Hey$_0$ → Hey$_{100}$) corresponds to $\Delta V = -78.73$ Å^2.

Using the data of Craig (1967), the net changes in unit-cell volume from cubic PbS to hypothetical cubic $Ag_{0.5}Bi_{0.5}S$ will be -33.61 Å^3 at room temperature. Finally, in the fizelyite – andorite series, full substitution from (hypothetical) $Pb_3Sb_2S_6$ (And$_0$) to andorite $PbAgSb_3S_6$ (And$_{100}$) produces a cell-volume change that can be estimated as -115.67 Å^3 (data of Kawada & Hellner 1971, Makovicky & Mumme 1983).

These values become comparable when divided by the respective unit-cell volumes. When real or hypothetical unit-cell volumes for the 50% Ag + Bi (Ag + Sb) substitution are used in the recalculation, the $\Delta V/V$ values will be -0.0412 Å^3 for 1 Å^3 of structure volume for the lillianite – gustavite solid solution, -0.04555 for the heyrovskyite solid solution, -0.1704 for the galena – matildite solid solution and -0.1025 for the andorite solid solution. Alternative calculations give -23.01, -15.75, -8.40 and -57.89 Å^3 per Pb atom replaced by ½Ag + ½ Bi (or ½ Sb in the last instance) in each of these structures.

For N = 11, interpolation of the above data for Ag–Bi–Pb sulfosalts indicates ΔV approximately

equal to -12.5 Å^3 for each Pb atom replaced. This means -112.5 Å^3 per unit cell for the whole substitution range from Our_0 to Our_{100}. The experimentally obtained difference of 60.82 Å between the unit-cell volumes of the exsolved phases thus equals 54.06% of the substitution range. For the Ag–Bi-rich minor exsolved phase, this indicates oversaturation equal to $68.5 + 54.1 = 122.6\%$, with the chemical formula $Pb_{-1.04}Ag_{5.52}Bi_{7.52}S_{13}$, *i.e.*, a clearly erroneous result.

If the exsolved phase is considered to be Our_{100}, $PbBi_{6.5}Ag_{4.5}S_{13}$, the observed difference in unit-cell volume ought to result from the substitution difference of only 31.5%; 2.82 Pb atoms would be replaced, with a volume change of -21.45 Å^3 per atom. If, as the other limiting alternative, a volume change of -57.84 Å per atom (which is known from the andorite solid-solution series) is considered, the cell-volume difference ought to represent the substitution difference of 11.68%, and the final substitution in the minor phase should amount to 80.18%, and its composition should be $Pb_{2.78}Ag_{3.61}Bi_{5.61}S_{13}$.

In order to resolve the ambiguity, point counting on a well-etched crystal of uniformly exsolved ourayite was undertaken. It yielded 26.33 vol. % for the minor phase which, after volume correction, gives 26.8 mol. %.

If the matrix is taken to represent $Our_{68.5}$, the composition of the exsolved phase can be calculated to be $Pb_{2.8}Ag_{3.6}Bi_{5.6}S_{13}$, *i.e.*, Our_{80}. It represents $Pb_{11.2}Ag_{14.4}Bi_{22.4}S_{52}$ in a unit cell, the closest integral compositions being $Pb_{12}Ag_{14}Bi_{22}S_{52}$ ($Our_{77.78}$), $Pb_{10}Ag_{15}Bi_{23}S_{52}$ ($Our_{83.33}$) and $Pb_8Ag_{16}Bi_{24}S_{52}$ ($Our_{88.89}$). The mass proportion of the minor phase would be 15.20 vol.% for the case of $Our_{88.89}$ and only 9.84 vol.% for the case of Our_{100} exsolving from the matrix. For $Our_{77.8}$, the two phases would exsolve in a 1:1 ratio.

The Two Varieties of Ourayite: A Summary

The present study indicates that at the temperature of formation, ourayite displays a limited range of solid solution along the line with constant *N*. This range contracts on cooling toward the ideal composition $Pb_4Ag_3Bi_5S_{13}$ ($Pb_{16}Ag_{12}Bi_{20}S_{52}$ in a unit cell), which represents $ourayite_{66.67}$. The natural compositions observed do not reach this value, being 68.5% for the matrix in the present study and 69.7% for the type ourayite from Ouray, Colorado. The above, new ideal formula is more plausible for the mineral at room temperature than the formula derived from the type material, which reads $Pb_{3.75}Ag_{3.125}Bi_{5.125}S_{13}$ (*i.e.*, $Pb_{15}Ag_{12.5}Bi_{20.5}S_{52}$), although the difference is small.

Like the type material, the ourayite from Ivigtut contains significant amounts of Cu, which was included in the calculations of the formula as isomorphic with Ag. This procedure brought the calculated *N* value closer to the ideal one. The above composition appears to favor a structurally asymmetrical chain of 11 octahedra in the galena-like slabs of the structure, and the second one of the two by systematic extinctions allow space groups *Bbmm* and $Bb2_1m$ (*cf.* Makovicky & Karup-Møller 1977a, Table 1).

The minor exsolved component represents ourayite with between 78 and 100% substitution, and most probably somewhat higher than 80%. Having a primitive unit-cell based on a pronounced *B*-centred subcell as well as a difference Δa (and not Δb) arising from exsolution in the parent higher-temperature ourayite, it stands closer to the members of the andorite – fizelyite series (the Pb–Ag–Sb sulfosalts) than to the other homologues of lillianite in the system Ag–Pb–Bi. The minor phase has apparently not attained full exsolution, being limited by its structural coherency with the matrix. For this reason, and also because of analytical problems and inability to apply the composition *versus* volume relationship observed in the lillianite homologous series, it is impossible to derive the ideal formula of the minor component. The preliminary (empirical) formula is $Pb_{2.8}Ag_{3.6}Bi_{5.6}S_{13}$, which represents $ourayite_{80}$. According to its crystallographic characteristics, it can be given the working name *P-ourayite* (*P* stands for primitive, uncentred) until additional compostional data on occurrences richer in Ag and Bi can be obtained in future. The type ourayite (*i.e.*, the matrix) then represents *B-centred ourayite.*

From the observations by X-ray diffraction and ore microscopy, the parallel exsolution of the two varieties of ourayite apparently proceeded as (100) lamellae of *P*-ourayite in the matrix of *B*-centred ourayite. However, the microscope observations suggest that this exsolution was apparently preceded by exsolution of broader lamellae (010) at somewhat higher temperatures. Both the (010) lamellae richer and poorer in Ag + Bi were later decomposed into the two room-temperature varieties along the (100) planes. The type specimen of ourayite from Colorado also displays indistinct (010) lamellae, but its original composition was closer to the ideal room-temperature composition, and no dissociation into the *P*- and *B*-centred varieties occurred.

In both deposits, ourayite is associated with the matildite – galena solid solution (about 68 mol% $Ag_{0.5}Bi_{0.5}S$). Thus, ourayite might represent the highest homologue of lillianite occurring as a primary phase under geological conditions.

Associated Minerals

The ore specimens exhibit ourayite as the major sulfosalt phase, associated with berryite, aikinite, galena, matildite, chalcopyrite, pyrite, native bis-

TABLE 3. AVERAGED MICROPROBE DATA FOR AIKINITE AND BERRYITE FROM IVIGTUT

Sample	Meas. points	Ag*	Cu*	Pb*	Bi*	S*	Total	Ag+	Cu+	Pb+	Bi+	S+	n_a	n_k
Aikinite														
191/76	4	0.0(0)	10.6(1)	32.7(4)	40.5(6)	17.4(6)	101.2(11)	0.0	32.1	30.5	37.4	104.8	82.3	17.7
29/78	4	0.0(0)	10.3(1)	31.9(8)	41.5(9)	17.8(3)	101.6(5)	0.0	31.5	29.9	38.6	107.9	77.1	22.9
30/78	9	0.1(2)	10.1(2)	32.5(5)	40.7(7)	17.8(4)	101.1(14)	0.1	31.1	30.7	38.1	108.9	78.9	21.1
Berryite														
191/76	2	6.8(1)	6.1(4)	21.3(6)	50.0(7)	17.5(0)	101.7(9)	12.6	19.2	20.5	47.7	109.0		
29/78	6	6.9(3)	6.3(1)	21.7(16)	49.2(15)	17.9(2)	102.0(13)	12.7	19.7	20.8	46.9	111.0		

Standard deviations are indicated in parentheses in terms of the last digit. * Data expressed in weight %. + Data expressed in atomic proportions, $\Sigma Me = 100$. n_a and n_k indicate the calculated percentage of aikinite-like and krupkaite-like ribbons, respectively, in the mineral examined.

muth, native gold and secondary minerals after aikinite. The Pb–Bi–Ag–Cu sulfosalts and galena were analyzed under the same analytical conditions as ourayite.

Berryite occurs as lamellar, randomly oriented grains in ourayite. It exhibits lamellar twinning and contains late galena, either exsolved from or replacing the mineral. In habit, it closely resembles berryite from the gustavite – cosalite – galena association (Karup-Møller 1966). The berryite that is associated with ourayite has the same chemical composition (Table 3) as that associated with eskimoite (Karup-Møller 1977).

Aikinite occurs as granular aggregates and equidimensional grains. Only occasionally does it exhibit lamellar development. The mineral is intergrown with ourayite, but the major portion lies isolated in the fine-grained fluorite – topaz association.

The analytical data on aikinite show that as in other occurrences (*cf.* the review by Makovicky & Makovicky, 1978, Fig. 1), its composition is rather far from the ideal end-member, $CuPbBiS_3$, and concentrates about the value with 80 atomic % of the aikinite end-member and 20 at.% of the krupkaite end-member (Table 3).

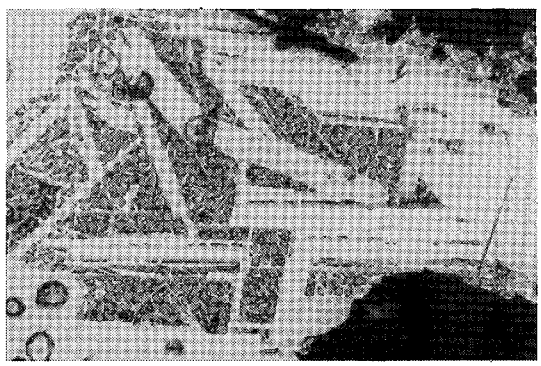

FIG. 6. Ourayite laths in etched galena matrix. Etched with concentrated HNO_3, plane-polarized light, 140×.

Aikinite is partly altered into a fine-grained heterogeneous mixture of gangue (or Bi-oxide ?), galena and an unidentified, strongly anisotropic sulfide called *mineral D* by Karup-Møller & Pauly (1979). Covellite and chalcopyrite may also be present. Aikinite in the fluorite – topaz material is generally much more altered than that associated with ourayite.

Galena is interstitial to laths of ourayite, extending from the margins of individuals grains of ourayite into their central areas. Ourayite laths may reside in the galena matrix (Fig. 6). In the case of berryite, galena occurs generally as numerous lenticular bodies enclosed in the mineral.

Galena associated with sulfosalts was analyzed for Ag and Bi (Table 4; see also Fig. 7). It is relatively enriched in Bi in comparison to Ag. The analyzed material spans the composition richest in Pb, with 94.7 at. % Pb, 3.9 at. % Bi and 2.4 at. % Ag, and the composition poorest in Pb, with 89.0 at. % Pb, 6.8 at. % Bi and 4.2 at. % Ag (metals normalized to 100%).

Matildite forms lamellar aggregates with interstitial galena, a typical decomposition product of the high-temperature solid solution $PbS–AgBiS_2$ (Fig. 8). Both components of the *galena – matildite* intergrowths were analyzed. *Matildite* represents the nearly pure end-member; the 0.2 at. % Pb (range 0.0–0.6 at. %) most probably comes from submicroscopic inclusions of galena. The slight excess of Bi observed in matildite may represent a microprobe artefact, similar to that in ourayite. The *galena* component lies on the $PbS–AgBiS_2$ join and has as average (metal-normalized) contents 4.2 (7) at. % Ag, 4.7(3) at. % Bi and 91.1(8) at. % Pb.

Four areas of the *galena – matildite intergrowths* with well-separated components (Fig. 8) were subjected to modal analysis by point counting. They yielded, respectively, 38.1, 36.4, 41.7 and 39.8 vol. % of the galena component. After the correction for unit-volume difference and for the Ag and Bi contents in the galena component, the percentage of matildite is, respectively, 68.9, 70.3, 65.7 and 67.3

TABLE 4. MICROPROBE DATA FOR GALENA AND MATILDITE FROM IVIGTUT

Mineral	Meas. points	Ag*	Bi*	Pb*	S*	Total	Ag+	Bi+	Pb+	S+
Galena[1]	5	1.9(4)	4.1(3)	80.2(13)	14.3(1)	100.6(9)	2.1	2.3	44.4	51.3
Matildite[1]	6	26.9(2)	53.4(5)	0.4(5)	18.0(1)	98.8(7)	23.4	23.9	0.2	52.5

		Ag*	Bi*	Ag*	Bi*	Ag*	Bi*
Galena[2]	12	1.93	6.07	1.62	3.80	1.68	4.34
		1.88	5.70	1.45	3.75	1.11	3.42
		1.80	4.56	1.43	3.80	1.71	4.56
		1.54	5.91	1.63	4.13	1.87	4.94

Standard deviations are indicated in parentheses in terms of the last digit. * Data expressed in weight %. + Data expressed in atomic %. 1. Components of the galena - matildite exsolution aggregate. 2. Galena associated with sulfosalts.

mol % $Ag_{0.5}Bi_{0.5}S$, the average being 68.1 mol. % $Ag_{0.5}Bi_{0.5}S$ and 31.9 mol. % PbS. The fine-grained "Widmanstätten structures" in some portions of the intergrowth could not be reliably analyzed by the methods available.

Native bismuth has only been observed in one polished section. It occurs as euhedral crystals that lie in isolation in black cryolite. Some crystals are partly decomposed along the margins.

Native gold occurs very seldom as inclusions in ourayite and is generally associated with chalcopyrite.

Chalcopyrite crystallized in patchy areas isolated in fluorite – topaz material or in contact with ourayite and associated minerals. It commonly contains euhedral crystals of ourayite (Fig. 9).

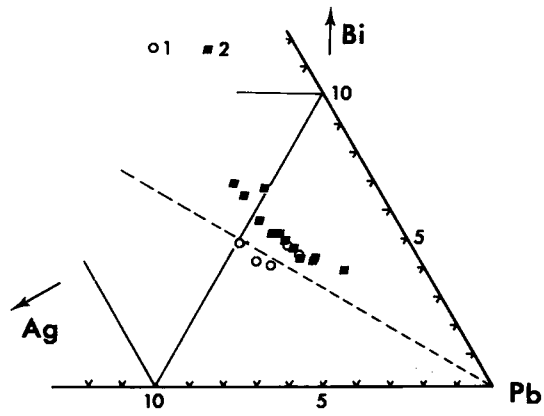

FIG. 7. Microprobe data for galena from Ivigtut in the compositional triangle Ag–Pb–Bi (in at. %). 1. Component of the galena – matildite intergrowth. 2. Galena associated with sulfosalts in sample 29/78.

ORIGIN AND MINERAL ASSOCIATIONS

The isolated fragments of the ourayite-bearing mineral association do not allow one to draw any firm conclusions about their position in the Ivigtut ore deposit or in the sequence of sulfosalt-containing associations. If the bulk of closely related gustavite – (vikingite –, eskimoite–) – cosalite – (aikinite–, berryite–) – galena associations from Ivigtut (Karup-Møller 1973, Karup-Møller & Pauly 1979) are taken into consideration, certain general conclusions become possible. Unlike ourayite, all of these associations were found *in situ* in the central parts of the deposit. Irregular tubular or podiform bodies, up to 20 cm in diameter, of fine-grained fluorite and topaz intergrown with gustavite or vikingite, or eskimoite, together with cosalite or aikinite and berryite, and with galena and other sulfides, are enveloped by a heterogeneous layer of fluorite (which includes a

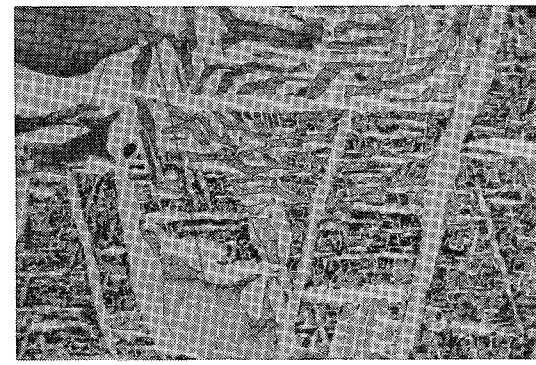

FIG. 8. Lamellar intergrowth of matildite and galena produced by the decomposition of the high-temperature $PbS–AgBiS_2$ solid solution. Etched, plane-polarized light, 380×.

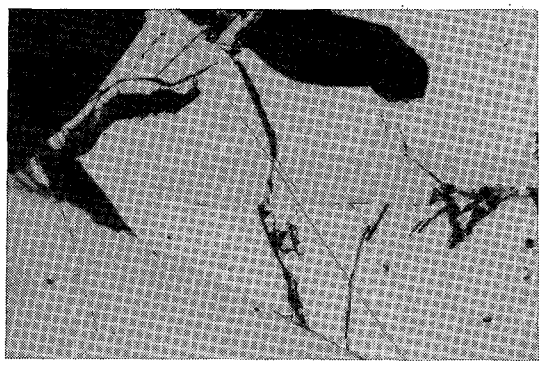

FIG. 9. Ourayite lath in chalcopyrite. Unetched, plane-polarized light, 120 ×.

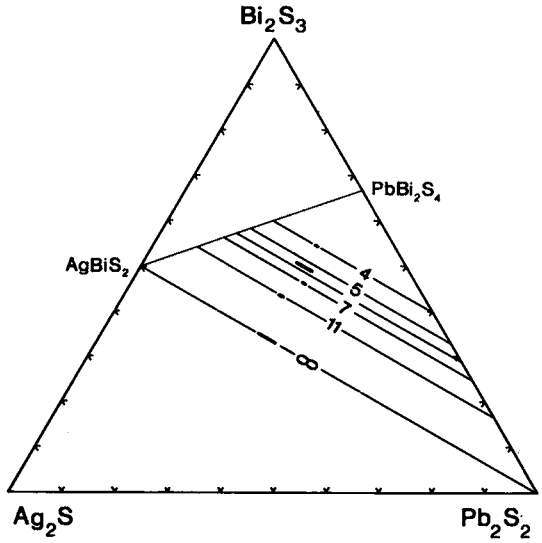

FIG. 10. Compositions of lillianite homologues from Ivigtut after Makovicky & Karup-Møller (1977b) and present work. Observed percentages of substitution (before exsolution, where applicable) and idealized N values are plotted. Overall constancy of the atomic Pb/(Ag+Bi) ratio is apparent from the plot.

brecciated generation), topaz, weberite, K-mica and pyrite.

The entire pocket was enclosed in massive siderite with a few percent of cryolite. At the sulfosalt locality, the massive sheet of siderite emerges from the quartz masses below the cryolite body and directly underlies the cryolite body (Karup-Møller & Pauly 1979, Fig. 2). The sulfosalt pocket occurs near the brecciated contact between this siderite sheet and the fluorite zone that separates the cryolite body from the underlying quartz body and was formed later than either of them. The materials of the pocket clearly suggest its affinity to the fluorite zone.

The structures observed in these sulfosalt associations suggest that they formed by filling and partial replacement of a porous, spongy and fractured aggregate of fluorite and topaz. Only rarely do the sulfosalt associations reach, replace or cement fractures in the minerals of the enveloping heterogeneous layer.

The ourayite association has a similar character, and it might represent the Ag-rich extrapolation of the associations just described. Its tentative localization suggests that further examples occurred in the Ivigtut deposit, although they went unnoticed. In the fluorite-enriched parts of the cryolite body and in similar mineralized breccias, the fine-grained galena – aikinite – primary matildite association was occasionally found without lillianite homologues.

It is not possible to determine the age relationships between the individual associations observed. The Bi-rich association may represent the oldest, and the matildite-containing assemblage the youngest association, in general agreement with the trends observed elsewhere (Karup-Møller 1977). The occurrence of almost all of them in a single large ore-pocket suggests that they might be nearly contemporaneous and connected with diffusion and crystalization processes in separate, poorly interconnected portions of the porous fractured gangue. All of the observed associations apparently represent late products associated with the formation of the fluorite body under the cryolite mass and of the fluorite-enriched parts in the cryolite body.

The lillianite homologues in the gustavite *etc.* sulfosalt associations display a remarkable compositional development. In order of decreasing Bi/Ag ratios, the homologues present in individual associations are gustavite (74.9; value before exsolution), vikingite (67.3 to 73.0), eskimoite (67.9) (all associated with Ag- and Bi-bearing galena) and ourayite (70.7 to 72.2; value before exsolution) associated with matildite (66 to 70). As Figure 10 shows, all the lillianite homologues lie (in the positions acceptable from a crystal-chemical point of view) in the zone with constant Pb/(Ag + Bi) ratio, with only the Bi/Ag ratio changing from one phase to another.

For the associations characterized by gustavite and vikingite, Ag- and Cu-bearing cosalite is typical. Berryite and aikinite are (preferentially) associated with eskimoite and ourayite. This suggests that copper was also accumulating concurrently with the increasing Ag/Bi ratio. Aikinite associated with eskimoite (Karup-Møller 1977, Table 10) represents aikinite (84.9) – krupkaite (15.1), very close to the aikinite described from the ourayite association in the present study.

ACKNOWLEDGEMENTS

The authors are greatly indebted to Mr. L. Andersen, Copenhagen, who donated the material for this study and to Professor H. Pauly, who forwarded it into our hands. Dr. J. Bailey and Prof. M.E. Fleet kindly commented on the manuscript. The principal research apparatus used came from several grants of the State Research Council of Denmark (Nat. Sci.).

REFERENCES

CRAIG, J.R. (1967): Phase relations and mineral assemblages in the Ag–Bi–Pb–S system. *Mineral. Deposita* **1**, 278-306.

HARRIS, D.C. & CHEN, T.T. (1975): Gustavite: two Canadian occurrences. *Can. Mineral.* **13**, 411-414.

KARUP-MØLLER, S. (1966): Berryite from Greenland. *Can. Mineral.* **8**, 414-423.

_____ (1970): Gustavite, a new sulphosalt mineral from Greenland. *Can. Mineral.* **10**, 173-190.

_____ (1973): A gustavite – cosalite – galena-bearing mineral suite from the cryolite deposit at Ivigtut, south Greenland. *Medd. Grønland* **195**(5), 1-40.

_____ (1977): Mineralogy of some Ag–(Cu)–Pb–Bi sulphide associations. *Geol. Soc. Denmark Bull.* **26**, 41-68.

_____ & MAKOVICKY, E. (1981): Ag- and Bi-rich heyrovskyite from the Bi–W–Mo mineralization at Castlegar, British Columbia. *Can. Mineral.* **19**, 349-353.

_____ & PAULY, H. (1979): Galena and associated ore minerals from the cryolite at Ivigtut, south Greenland. *Medd. Grønland, Geosci.* **2**, 3-25.

KAWADA, I. & HELLNER, E. (1971): Die Kristallstruktur der Pseudozelle (subcell) von Andorit VI (Ramdohrit). *Neues Jahrb. Mineral. Monatsh.*, 551-560.

KLOMÍNSKÝ, J., RIEDER, M., KIEFT, C. & MRÁZ, L. (1971): Heyrovskýite, $6(Pb_{0.86}Bi_{0.08}(Ag,Cu)_{0.04})S{\bullet}Bi_2S_3$ from Hůrky, Czechoslovakia, a new mineral of genetic interest. *Mineral. Deposita* **6**, 133-147.

MAKOVICKY, E. (1977): Chemistry and crystallography of the lillianite homologous series. III. Crystal chemistry of lillianite homologues. Related phases. *Neues Jahrb. Mineral. Abh.* **131**, 187-207.

_____ & KARUP-MØLLER, S. (1977a): Chemistry and crystallography of the lillianite homologous series. I. General properties and definitions. *Neues Jahrb. Mineral. Abh.* **130**, 264-287.

_____ & _____ (1977b): Chemistry and crystallography of the lillianite homologous series. II. Definition of new minerals: eskimoite, vikingite, ourayite and treasurite. Redefinition of schirmerite and new data on the lillianite – gustavite solid-solution series. *Neues Jahrb. Mineral. Abh.* **131**, 56-82.

_____ & MAKOVICKY, M. (1978): Representation of composition in the bismuthinite – aikinite series. *Can. Mineral.* **16**, 405-409.

_____ & MUMME, W.G. (1983). The crystal structure of ramdohrite $Pb_6Sb_{11}Ag_3S_{24}$, and its implications for the andorite group and zinkenite. *Neues Jahrb. Mineral. Abh.* **147**, 58-79.

SPRINGER, G. (1967): Die Berechnung von Korrekturen für die quantitative Elektronenstrahl-Mikroanalyse. *Fortschr. Mineral.* **45**, 103-124.

SWEATMAN, T.R. & LONG, J.V.P. (1969): Quantitative electron-probe microanalysis of rock-forming minerals. *J. Petrology* **10**, 332-379.

VENDRELL-SAZ, M., KARUP-MØLLER, S. & LOPEZ-SOLER, A. (1978): Optical and microhardness study of some Ag–Cu–Pb–Bi sulphides. *Neues Jahrb. Mineral. Abh.* **132**, 101-112.

Received May 5, 1983, revised manuscript accepted March 17, 1984.